AADE-14-FTCE-62

A Study of geometric non-conventionalities of a commercial desilter

Curt M. A. Panisset and André L. Martins, Petrobras; Marcos A. Souza Barrozo and Carlos H. Ataíde, Federal University of Uberlândia.

Abstract

This paper is a study on hydrocyclones, a solid-liquid separation device that integrates the solid control system and, in the field, is known as desilter. The purpose of this work was to determine the effect of non-conventionalities that can be found in commercial equipment that is used on a drilling rig. These peculiar geometric characteristics are: the change in the transversal section of the feed chamber from circular to rectangular; the presence of a feeding ramp; and a conical section with two angles. The study of the non-conventionalities was carried out using a suspension of phosphate concentrate at the volumetric concentration of 1% in water.

Introduction

When drilling an oil well, the rock is worn by a drill bit and because of that, drill cuttings are generated. These must be removed from the well so that the drilling may occur without problems. Such removal is accomplished by a fluid, known as tdrilling fluid. This fluid has other functions besides cleaning the well. So, in order for the drilling fluid to perform its functions, it has to maintain certain properties such as density, viscosity, filtered volume and thickness of the wall cake. To achieve the control of these properties, a solid-liquid separation plant, known as the solids control system, is employed in order to remove the drilled cuttings from the drilling fluid.

The vibrating screens, known as shale shakers, the hydrocyclones, known as desanders and desilters and the decanter centrifuges are the most common equipment applied in the solids control system.

The desilters are non-conventional hydrocyclones and the diameter of its cylindrical part range from four to six inches. They are employed with the intention of removing drilled solids with dimensions of fifteen to thirty-five micrometers. This particle size range corresponds to silt, hence the name desilter.

Normally the desilters are used in batteries ranging from eight to sixteen cones. The processing rate for each desilter ranges from fifty to seventy-five gallons per minute (gpm), and they began to be used around 1962 to remove the silt present in the drilling fluid. Particles of this size usually affect greatly the efficiency of the mud cake. As a consequence of this, a drastic reduction in differential sticking occurred [1].

The hydrocyclone technology is very interesting because it has a small size compared to other types of separators, has no moving parts, presents a low cost of installation and operation, has no need of a dedicated operator and has operational flexibility [2].

Hydrocyclones consist of an upper cylindrical body joined by a conical section opened at its end. The lower end orifice in the cone is known as apex (Figure 1). The liquid containing the particles to be separated is fed into the hydraulic cyclone by a centrifugal pump. The feed nozzle directs the flow to the top of the cylindrical body at high velocity. This causes the mixture to acquire a helical movement downward. This swirling motion generates a centrifugal force due to the curvilinear trajectory, driving the solids to the wall, consequently separating the two phases. The feed nozzle may be tangential to the cylinder wall or in the form of a volute.

The reduction in diameter of the conical section results in a gradual increase of the centrifugal force, and it causes a gain in separation efficiency. On the wall of the equipment the liquid with a concentrated amount of solid ends up being discharged through the apex. This current is called underflow. The central part of the flow undergoes a change in the direction of movement and starts to move towards an outlet at the top of the cylindrical part (the vortex finder). This current is called overflow. The flow pattern present on the

inside of the device can be seen in Figure 2 [3]. The upward movement of fluid generates a low pressure zone in the center of the hydrocyclone that sucks air through the apex, generating an air filled volume known as air core [4].

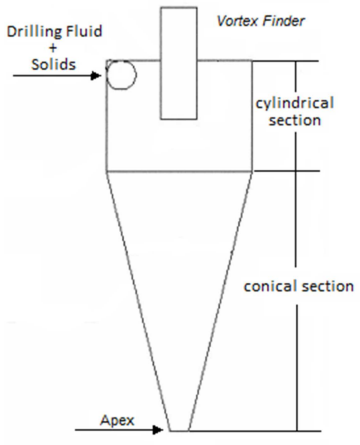

Figure 1. Schematics of a hydrocyclone.

Although the operation of a hydrocyclone and the flow pattern described above are easy to understand, the force and velocity fields established are extremely complex [2].

The performance of this type of equipment is closely related to the geometric proportions of its dimensions. Thus, changes in the dimensions of the geometric variables, such as height of the cylindrical part, angle of the conical section, diameter of the feed nozzle, apex and the vortex finder influence significantly in the performance of the equipment [5].

The objective of this work was to study the non-conventionalities of a commercial desilters used on the drilling rigs. The studied equipment can be seen in Figure 3. The model chosen for this study has a characteristic diameter of 4 inch (101.6 mm). The peculiar geometric characteristics that make this a non-conventional equipment are: a conical section with two angles, one of 28° and another of 16,5° (Figure 3); the change in the feed duct´s cross section from circular to rectangular (see Figure 4); and the presence of a feeding ramp (see Figure 4).

In Figure 4, a cut of the top of the studied hydrocyclone is shown, but it is upside-down. In this image, one can see the vortex finder, the feeding ramp and the cross sectional area of the feed going from circular to rectangular.

The change in the cross section of the feed reshapes the flow profile so that the incoming drilling fluid may adapt its flow to the feed chamber. This increases the processing rate of the device and the separation efficiency [1]. The use of a feeding ramp forces the incoming flow downward in such a manner that the fluid which has completed the first turn does not collide with the fluid that is entering the hydrocyclone. This minimizes turbulence and increasing the processing flow rate and separation efficiency [1].

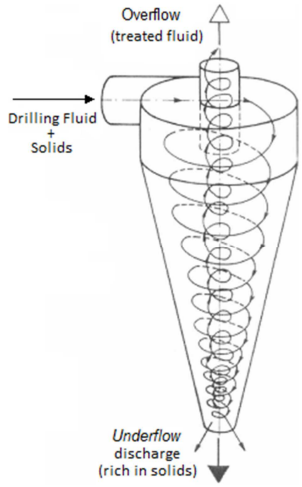

Figure 2. Hydrocyclone flow pattern (figure adapted from reference [3]).

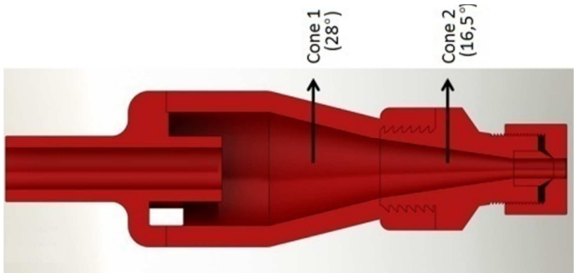

Figure 3. Cut on the equipment showing the cone with two different angles.

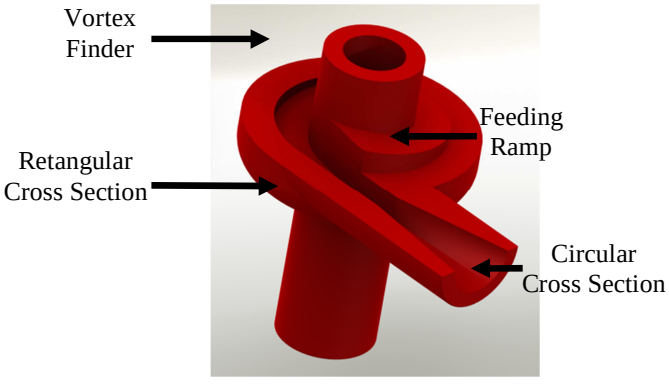

Figure 4. A cut on the top of the studied hydrocyclone showing the change in cross sectional area and the feeding ramp.

Methodology

Studied hydrocyclone:

A replica of the field equipment was built in a scale of 1:3,4. The diameter of the cylinder assumed the value of 30 mm. This scaled-down replica was extruded in polyurethane in a modular fashion. Five pieces were manufactured: the overflow duct and vortex finder (Part 1), a piece of adaptation, so that the feed ramp could be used (Part 2); the cylindrical part containing feed duct (Part 3) ; the conical portion (Part 4); and underflow (Part 5). The assembled hydrocyclone with all of its pieces can be seen in Figure 5.

Its dimensions are: diameter of the cylindrical part (DC) equals 30 mm, height of the cylindrical part (h) of 37 mm, the cross sectional area of the supply duct (AI) 41.8 mm^2. The first cone with the cone height (H1) of 29.5 mm and angle (θ1) of 28° and the second cone with height (H2) of 39.4 mm and 16.5 º angle (θ2); apex diameter (OD) of 5 mm and a height of 16 mm; vortex finder internal diameter (OD) equal to 10.8 mm and a length (L) of 23.5 mm.

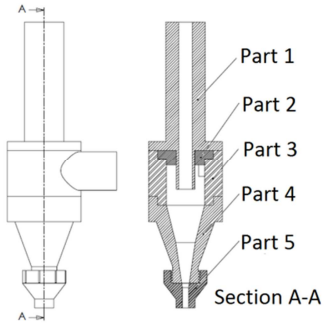

Figure 5. Schematics of the scaled down model.

The assembled equipment using part 2 has no feed ramp. A feed ramp itself was built as a different piece and can be assembled as a substitute for Part 2. The part containing the feed ramp is shown in Figure 6.

Figure 6. Part used to insert the feed ramp on the scaled down hydrocyclone.

Two other pieces were built. One piece is equivalent to part 3, but its feed duct did not change the cross sectional area from circular to rectangular. And one piece is equivalent to part 4, but present only one angle, 22°.

Since the equipment is modular, it can be assemble in eight different settings. The equivalent field equipment has the change in the cross sectional area of the inlet duct, a feed ramp and two cone angles. It will be referred as RP2 (at Table 1,highlighted in green). A conventional hydrocyclone would have a circular feeding duct, no feed ramp, and only one cone. It will be called CA1 (at Table 1, highlighted in blue). All possible combinations and its acronyms are shown in Table 1.

Table 1. All possible configurations of the studied hydrocyclone.

Acronym	Inlet	Ramp	n° of cones
RP2	**R**ectangular	**P**resent	2
RP1	**R**ectangular	**P**resent	1
RA2	**R**ectangular	**A**bsent	2
RA1	**R**ectangular	**A**bsent	1
CP2	**C**ircular	**P**resent	2
CP1	**C**ircular	**P**resent	1
CA2	**C**ircular	**A**bsent	2
CA1	**C**ircular	**A**bsent	1

Experimental Unit:

The experimental apparatus used for the tests can be seen in Figure 7. The mixture to be separated was stored in a tank containing a cooling unit (10) to minimize the heating of the mixture and an agitator to maintain the solid material suspended (4).

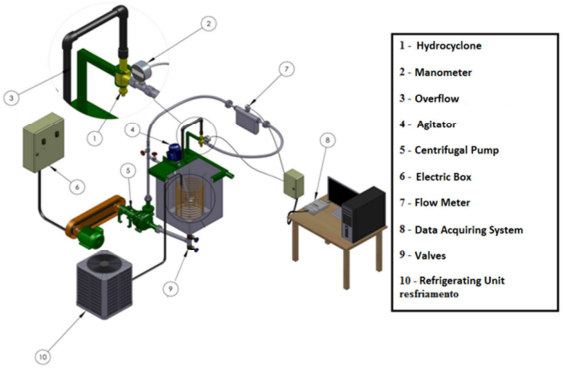

Figure 7. Schematics of the experimental unit.

A tube leaving from the bottom of the tank takes the fluid to a 10 hp centrifugal pump (5). The pump discharges the mixture at tube that leads to the hydrocyclone and also

contains a bypass. Before going to the hydrocyclone the mixture flowed through a Coriolis flow meter (7) and a manometer (2). The flow information and pressure value were registered by a data acquiring system. Each measurement lasted 10 s at a measuring rate of 1,000 points per second. The mean and standard deviation of these measures were stored.

Material Characterization:

The experimental tests were carried out using 160 L of a suspension of phosphate concentrated at the volumetric concentration of 1% in water. The phosphate rock had a density of 3.27 g/cm3 (determined by Helium pycnometry using the Accupyc Micrometrics 1330). Furthermore, the Particle Size Distribution (PSD) of it was evaluated by laser diffraction (Malvern Mastersizer 2000). The Rosin, Rambler e Bennett model (RRB) for size distribution was applied and its parameters were a "n" of 0.745 and d63.2 of 23 micrometers.

Experimental Procedure:

Using the bypass valve, the mixture was directed to the hydrocyclone at a pressure of 75 psi. After the flow was stable, the mass flow rate of the feed pressure, overflow and underflow, were measured three times. The measurement of the underflow mass rate was carried out weighting the collected underflow over a period of time. The other two measures were made by the data acquiring system.

Six samples from each flow stream were collected. Three were used for PSD analysis by laser diffraction (Mastersizer 2000) and the other three samples were used for gravimetric determination of the phosphate's mass concentrations.

The same procedure was repeated for the feed pressures of 50 to 25 psi, in that particular order.

Results and discussion

Processing Flow Rates (W):

The results of Pressure (P) and Mass Flow Rates (W) at the three flow conditions and for each configuration are shown in Table 2. Each measure was taken three times and each one is the average of 10, 000 measurements. So the values are the average of a total of 30,000 measurements. The standard deviations for W (Mas Flow Rate) ranged from 6 to 7 g/s and for P (Pressure) ranged from 0.1 to 0.4 psi. Thus, from the statistical point of view, RP1 and RP2 present an identical value of Mass Rate for the pressure of 25 psi (W3).

Analyzing the results, it can be seen that the hydrocyclones RP2 and RP1 have the biggest processing flow rate for 25 and 50 psi but, at 75 psi the biggest W belongs to RP1. The configuration that present the smallest W for all conditions is CA2 and CA1.

Table 2. Results of flow rates and pressures for each configuration. Pressure is in psi and mass flow rate is in g/s.

Acronym	P1	W1	P2	W2	P3	W3
RP2	75.6	679	49.7	557	24.9	396
RP1	74.2	700	50.4	561	25.5	392
CP2	75.8	639	50.3	519	25.3	364
CP1	75.1	616	50.4	537	25.5	366
RA2	75.5	523	50.4	424	25.4	300
RA1	75.2	529	50.2	431	24.9	304
CA2	75.4	516	50.1	415	25.4	297
CA1	75.4	516	50.5	420	25.5	299

For all configurations an increase in pressure leads to an increase in flow rate. The most drastic gain comes from RP2 and RP1.

The effect of the feed duct type:

Figure 8 brings the graphics of W for each P and all configurations. The blue columns are the W referent to 25 psi, the red are the W of 50 psi and green the 75 psi. The graphic is organized in such a way that each pair of columns shows one configuration with a change in the inlet duct and its equivalent without the change in the inlet duct. This way they can be compared directly. The horizontal lines work as a reference to compare the height of each group of columns.

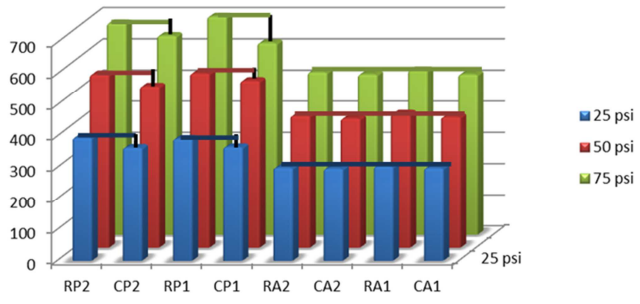

Figure 8. Mass flow rate (g/s) of all configurations for each pressure (psi) focusing the type of inlet duct.

As it can be seen in Figure 8, when the inlet duct

does not have the transition from circular to rectangular, the processing flow rate is reduced if the feed ramp is present. This is occurs for all the pressures, so W for RP2 is smaller than the one for CP2 and the for RP1 is smaller than the one for CP1. When the feed ramp is not present (RA2, CA2, RA1 and CA1) the mass flow rate is almost constant for all the configurations.

The effect of the feed ramp:

Figure 9 brings the graphics of W for each P and all configurations. The blue columns are the W referent to 25 psi, the red are the W of 50 psi and green the 75 psi. The graphic is organized in such a way that each pair of columns shows one configuration with a feed ramp and its equivalent without it. This way they can be compared directly. Again, the horizontal lines work as a reference to compare the height of each group of columns.

As it can be seen in Figure 9 for all the pressures (25, 50 and 75 psi) when the ramp is not present the processing flow rate is reduced drastically for all pairs of configuration.

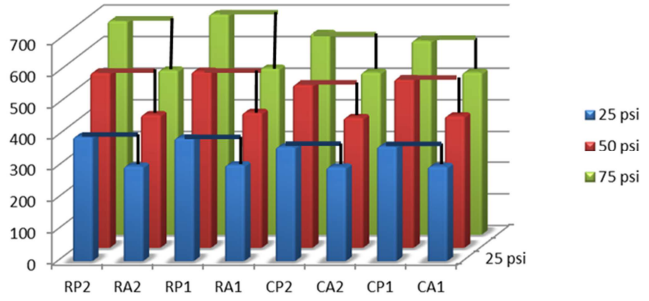

Figure 9. Mass flow rate (g/s) of all configurations for each pressure (psi) focusing the presence or absence of the feed ramp.

The effect of the cone type:

Figure 10 brings the graphics of W for each P and all configurations. The graphic is organized in such a way that each pair of columns shows one configuration with two conical sections (two angles) and its equivalent with only one. Once more, the horizontal lines work as a reference to compare the height of each group of columns.

As it can be seen in Figure 10 the presence of one or two angles are statically identical for every pair of configurations and in any pressure.

Separation Efficiency:

The results of the Separation Efficiency (η) at the three flow conditions and for each configuration are shown in Table 3. The measurement follows the same protocol as explained in the previous section.

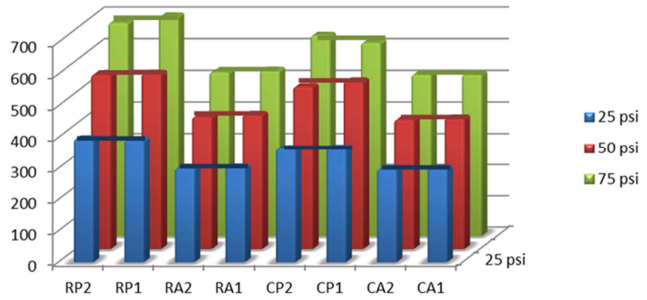

Figure 10. Mass flow rate (g/s) of all configurations for each pressure (psi) focusing in the type of cone.

η is defined as the coefficient of the solids mass flow rate of the underflow (W_{SU}) and the solids mass flow rate of the feeding stream (W_S) and it can be calculated using Eq. 1.

$$\eta = \frac{W_{SU}}{W_S} = \frac{Q_U C_{VU}}{Q C_V} \quad (1)$$

Where Q_U and Q are the volumetric flow rate of the underflow and of the feeding stream and C_{VU} and C_V is the volumetric concentration of solids in the underflow and on the feeding stream.

At Table 3 it can be observed that for the pressure of 25 psi, all configurations with no feed ramp have a similar η, and higher than the ones that present the ramp. For the other pressures pressure (50 and 75 psi) the biggest efficiency is given by CA2. The smallest η from all the pressures come from CP2.

In all cases, except RA2, the increase in pressure resulted in an increase in η.

The effect of the feed duct type:

Figure 11 brings the graphics of η for each P and all configurations. The graphic is organized in such a way that each pair of columns shows one configuration with a change in the inlet duct and its equivalent without the change in the inlet duct. This way they can be compared directly. The horizontal lines work as a reference to compare the height of each group of columns.

The effect of the feed duct type:

Figure 11 brings the graphics of η for each P and all configurations. The graphic is organized in such a way that each pair of columns shows one configuration with a change in the inlet duct and its equivalent without the change in the inlet duct. This way they can be compared directly. The horizontal lines work as a reference to compare the height of each group of columns.

Table 3. Results of separation efficiency for each pressure and all configurations. Pressure is in psi and separation efficiency (η) in %.

Acronym	P1 (75 psi)	P2 (50 psi)	P3 (25 psi)
RP2	77.3	65.8	62.5
RP1	75.5	70.7	67.2
CP2	62.2	60.7	59.3
CP1	72.5	64.8	64.3
RA2	70.8	69.8	71.7
RA1	75.6	72.7	71.8
CA2	82.1	75.4	69.3
CA1	76.2	73.0	70.6

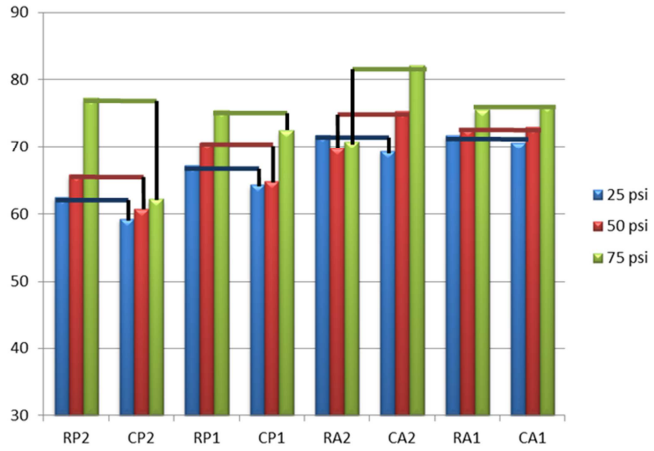

Figure 11. η (%) of all configurations for each pressure (psi) focusing the type of inlet duct

At the pressure of 25 psi the rectangular ending is always positive. As for the other pressures, when the ramp is present (the first four columns) the presence of a rectangular inlet duct results in an increase in η. In the case of RA2 and CA2, the change of cross sectional area in the feed duct is responsible for a decrease in η. For RA1 e CA1 the change in the cross sectional area has little relevance.

The effect of the feed ramp:

Figure 12 brings the graphics of η for each P and all configurations. The graphic is organized in such a fashion that each pair of columns show one configuration with a feed ramp and its equivalent without it.

As it can be seen in Figure 12 for almost all the pressures when the ramp is present the η is reduced drastically for all pairs of configuration. The two exceptions are at the pressure of 75 psi where RP1 and RA1 that have a similar η and RP2 that presents a higher η than RA2.

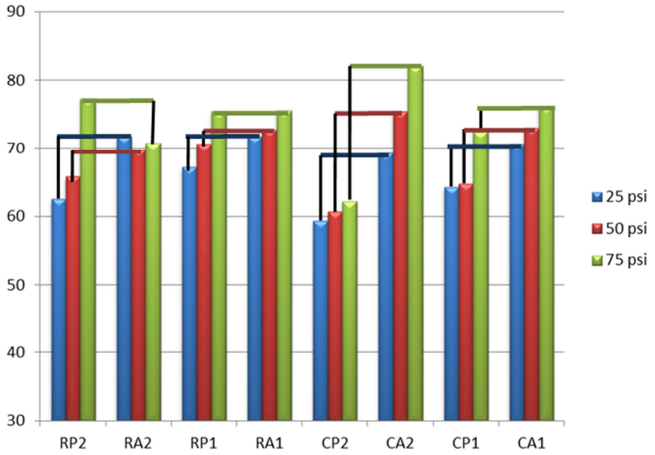

Figure 12. η (%) of all configurations for each pressure (psi) focusing the presence or absence of the feed ramp.

The effect of the cone type:

Figure 13 brings the graphics of η for each P and all configurations. The graphic is organized in such a way that each pair of columns shows one configuration with two conical section (two angles) and its equivalent with only one.

In general the presence of two angles at the conical section is responsible for a reduction on the η. For the pairs RA2/RA1 and CA2/CA1 at 25 psi the η are similar. For RP2/RP1 and CA2/CA1 at 75 psi the use of two angles is beneficial.

Underflow Liquid Ratio (LR):

The underflow fraction of liquid, or Liquid Ratio (*LR*) is defined as the coefficient of the liquid mass flow rate of the underflow (W_{LU}) and the liquid mass flow rate of the feeding stream (W_L) and it can be calculated using Eq. 2.

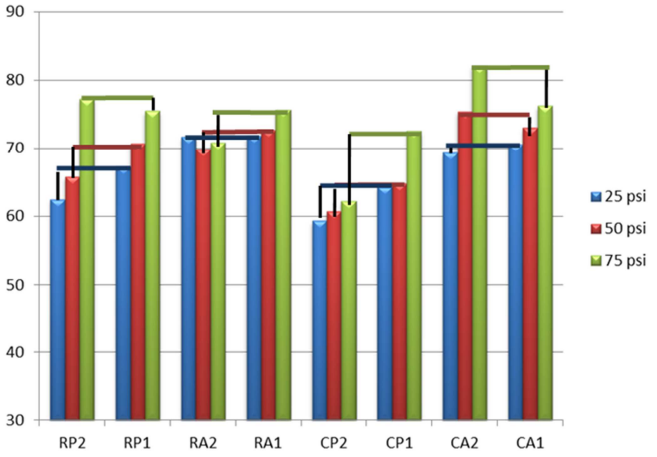

Figure 13. η (%) of all configurations for each pressure (psi) focusing in the type of cone.

$$LR = \frac{W_{LU}}{W_L} = \frac{Q_{LU}}{Q_L} \qquad (2)$$

Where Q_{LU} is the volumetric flow rate of liquid in the underflow stream and Q_L is the volumetric flow rate of liquid in the feeding stream. Results of the Liquid Ratio (*LR*) at the three flow conditions and for each configuration are shown in Table 4.

For all pressures the highest *LR* is the one from RP1 and the smallest one is the one from RA2. And, in general, the *LR* tends to increase with an increase in pressure.

Table 4. Results of *LR* for each pressure and all configurations. Pressure is in psi and *LR* in %.

Acronym	P1 (75 psi)	P2 (50 psi)	P3 (25 psi)
RP2	6.18	5.13	4.18
RP1	14.36	12.72	12.38
CP2	10.63	10.03	9.42
CP1	10.89	9.19	9.82
RA2	3.29	3.50	3.93
RA1	5.71	4.96	4.63
CA2	5.03	5.04	3.50
CA1	6.29	5.05	3.97

In general, LR above 7% is not acceptable, because the underflow is to be directed to discharge and the drilling fluid is too expensive. In order to recuperate part of the underflow this stream is generally directed to a dedicated shale shaker but it´s screen have such a high mesh that its processing flow rate is really small. Because of this, the configurations RP1, CP2 and CP1 are not to be considered.

The effect of the feed duct type:

Figure 14 brings the graphics of LR for each P and all configurations. The graphic is organized in such a way that each pair of columns show one configuration with a change in the inlet duct and its equivalent without the change in the inlet duct. This way they can be compared the LR´s directly. The horizontal lines work as a reference to compare the height of each group of columns.

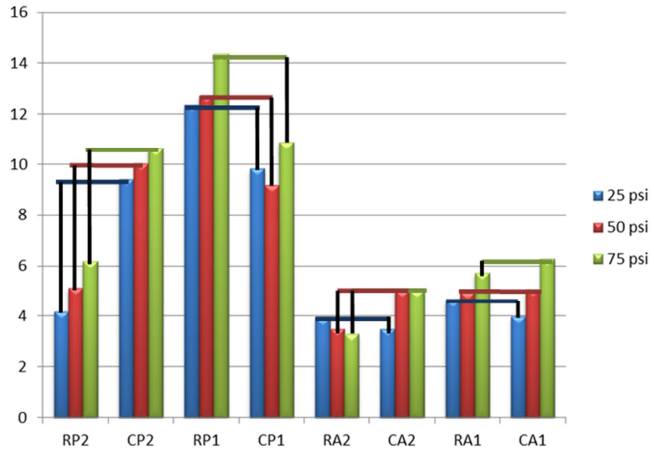

Figure 14. LR (%) of all configurations for each pressure (psi) focusing the type of inlet duct

Figure 14 it is hard to conclude anything by analyzing the relationship between the change in the inlet duct and the behavior of the *LR*.

The effect of the feed ramp:

Figure 15 brings the graphics of *LR* for each P and all configurations. The graphic is organized in such a fashion that each pair of columns show one configuration with a feed ramp and its equivalent without it.

As it can be seen in Figure 15 the use of a feed ramp increases the *LR* in all cases except for the pair RP2/RA2 at the pressure of 25 psi.

The effect of the cone type:

Figure 16 brings the graphics of *LR* for each P and all configurations. The graphic is organized in such a way that each pair of columns show one configuration with two conical section (two angles) and its equivalent with only one.

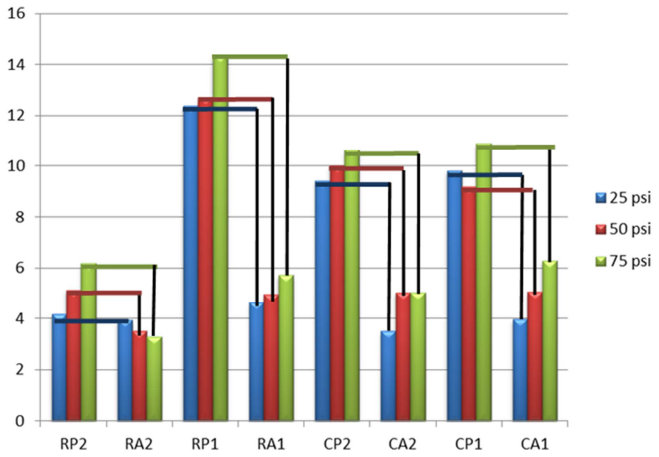

Figure 15. LR (%) of all configurations for each pressure (psi) focusing the presence or absence of the feed ramp.

In general the presence of two angles at the conical section is responsible for a reduction on the *LR*.

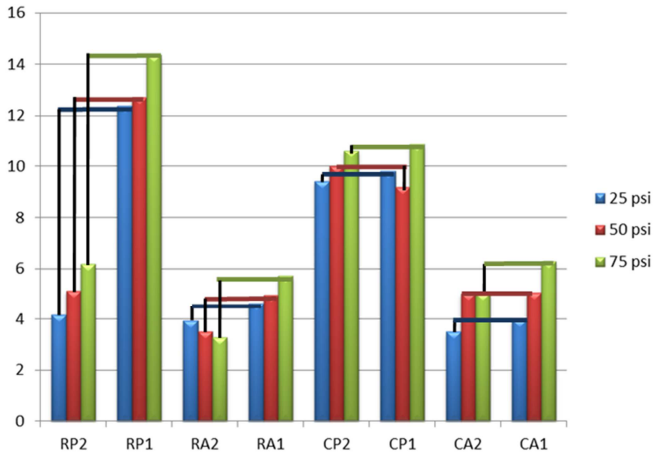

Figure 16. *LR* (%) of all configurations for each pressure (psi) focusing in the type of cone.

Conclusions

About the effects of each non conventionality, it is clear that the rectangular shape of the inlet duct results in an improvement on the processing flow rate when the ramp is present. This can also be observed about the efficiency. So, whenever using the ramp it is beneficial to employ the rectangular cross section in the feeding duct.

The use of the feed ramp improves the processing capacity, and leads to a loss of efficiency and a worst Liquid Ratio.

The use of the rectangular inlet and two angles cancel out the effect that the feed ramp has on the LR and all three characteristics together leads to a smaller efficiency and a bigger processing rate with an acceptable LR.

It is interesting to start the overall conclusions by the *LR*. As it was said, values bigger than 7% are not acceptable, so, the configurations RP1, CP2 and CP1 have no practical application.

The RP2 is the field model, so it can be used as a standard to compare the performance of the other four configurations.

If the *LR* is taken into account the best configuration is RA2, in second place CA2 and the others are statistically together in third place (RP2, RA1 and CA1).

If the *W* is taken into account the best configuration is the field configuration (RP2). All the others are statistically together in second place. Because of this it can be deduced that this model was optimized in order to give the best processing rate but maintaining the *LR* within an acceptable rage.

If the η is taken into account the best configuration is CA2. If the pressure is 25 or 50 psi the configurations without the ramp are in second place, but for 75 psi the field configuration takes the second position.

The feeding pressures used in the field are close to 50 psi. If this pressure is taken as a reference we have three interesting configurations, RP2 (the one already used in the field), CA1 (the conventional hydrocyclone) and CA2. They all have equivalents LR.

RP2 can process 32 % more fluid than CA1 (already in use).

CA2 have a η 14 % bigger than RP2 (would have to be manufactured).

An oilwell is drilled in phases. A typical pump rate of a first phase with return to the surface in deep water drilling ($17^1/_2$") is 1200 gallons per minute (gpm) and RP2 is capable of handling this. But, on the second and third phases the pump rates are 800 and 400 gpm. These pump rates are compatible with the processing capability of CA2. So, when the first phase ends it is possible to exchange the RP2 for CA2. This way the pump rate could be managed and separation would work at a higher efficiency.

So it would be interesting to manufacture a CA2 with a characteristic diameter of 4 inch to test it in the field.

Another observation is the fact that the increase in

pressure to 75 psi can increase the efficiency considerably. So it would be interesting to check if the desilter systems that are already installed on the rigs could operate at higher pressures. If so, a study should be carried out to determine the increase of efficiency resulting from this increment on the working pressure. If not, establish a technical and economic study in order to determine whether it is interesting to install a new system capable of operating at higher pressures.

Acknowledgments

The authors acknowledge the financial support provided by PETROBRAS.

References

[1] ASME (American Society of Mechanical Engineers), Shale Shaker Committee, “Drilling fluid processing handbook”, United States of America, Gulf Professional Publishing, pp. 1-13 e 257-281, 2005.

[2] L.G.M. Vieira, “Otimização dos processos de separação em hidrociclones filtrantes”, Tese de doutorado, Uberlândia, pp. 1-54, Maio 2006.

[3] R.A. Medronho, J. Scuetze, W. D. Deckwer, “Numerical simulation of hydrocyclones for cell separation”, Latin American Applied research, v 35, n. 1ann, Bahia Blanca, março, 2000, (http://www.scielo.org.ar/scielo.php?script=sci_arttext&pid=S0327-07932005000100001).

[4] C.M.A. Panisset, M.P. Mendonça, R.B. Silva, C.R. Duarte, C.H. Ataíde, “Estudo da influência de diferentes configurações na alimentação de um hidrociclone do tipo dessiltador através de técnicas de CFD”, IV Encontro Nacional de Hidráulica de Poços de Petróleo e Gás, Foz do Iguaçu, PR, Brazil, agosto, 2011.

[5] F.S. Lobato, L.G.M. Vieira, M.A.S. Barrozo, “Estudo do desempenho de hidrociclones usando a metodologia de superfície de respostas e otimização multi-objetivo”, XIV Encontro de modelagem computacional, Nova Friburgo, RJ, Brazil, novembro, 2011.